Principles and current trends in the correlative evaluation of glioma with advanced MRI techniques and PET

Spyridon Tsiouris MD, PhD,
Charalampos Bougias RT, MSc,
Andreas Fotopoulos MD, PhD

Department of Clinical Nuclear Medicine,
University Hospital of Ioannina,
Stavros Niarchos Avenue, Ioannina 45500, Greece

Keywords: Glioma
-Perfusion-weighted MRI
-Diffusion-weighted MRI
-MR spectroscopy
-Amino acid PET -^{18}F-FET
-^{18}F-FDOPA -^{11}C-MET

Corresponding author:
Spyridon Tsiouris MD, PhD,
Department of Clinical Nuclear Medicine,
University Hospital of Ioannina,
Ioannina 45500, Greece,
Phone: +30 26510 99379,
spytsi@gmail.com

Received:
26 August 2019
Accepted revised:
14 October 2019

Abstract
Cerebral gliomas comprise a heterogeneous group of primary neoplasms of the central nervous system, representing a significant cause of cancer morbidity and mortality. Contrast-enhanced magnetic resonance imaging (MRI) is paramount for identifying structural brain abnormalities related to the development of gliomas. Although morphological MRI remains the current standard of care for initial diagnostic workup, surgical planning, monitoring therapy response and surveillance during follow-up, it is rather difficult to define tumor grade and boundaries and to assess response to radiochemotherapy solely by contrast-enhancement, due to a variety of factors influencing blood-brain barrier (BBB) permeability and contrast agent distribution. The nature of a lesion lies beyond often misleading gross structural patterns, down to the cellular and molecular level, hence the imaging techniques of advanced multimodal MRI and positron emission tomography (PET) have emerged to provide critical non-invasive insight into the underlying biology of primary brain cancer. Out of the various PET radiotracers, labeled amino acids are of particular significance due to their non-dependency on BBB disruption to reach glioma cells and their excellent tumor-to-background contrast. After discussing the basic imaging principles of MR perfusion, diffusion, spectroscopy and PET in glioma, this review focuses on the correlative imaging with amino acid PET and advanced MRI techniques in tumor grading and staging, in guiding stereotactic biopsy and surgical excision and in assessing therapy response, post-therapy surveillance and prognosis. Lastly, a reference is made on the expanding availability of integrated PET/MRI systems and the resulting benefits of simultaneous image acquisition.

Hell J Nucl Med 2019; 22(3): 206-219 *Published online: 30 October 2019*

Introduction

With an annual incidence rate of 5-6 cases per 100,000 of population worldwide, cerebral gliomas account for approximately 24% of primary brain tumors in adults and as a group is the second most frequent intracranial tumors (after meningiomas), representing a significant cause of cancer morbidity and mortality [1].

According to the World Health Organization (WHO) classification scheme, gliomas are categorized histologically into astrocytomas (AS), oligodendrogliomas (OD), ependymal tumors and tumors of the choroid plexus and are assigned a grade (I through IV), based on their predicted biological behavior [2]. Grades I & II are low-grade gliomas (LGG) and include low-grade AS and low-grade OD; grades III & IV are high-grade gliomas (HGG) and include anaplastic AS and anaplastic OD (grade III) and glioblastoma multiforme (GBM) (grade IV). Up until a few years ago, gliomas were classified solely by histology. Building on advances in molecular genetics and the development of epigenetic profiles, the WHO revised their classification system in 2016 to incorporate molecular criteria such as IDH mutation and 1p/19q co-deletion along with histology, in an effort to more accurately diagnose, prognosticate, predict treatment efficacy and enhance individualized therapy planning [3].

Radical surgical excision is usually curative in benign tumors. Treatment options for HGG entail maximal safe surgical resection of the tumor bulk, followed by 6 weeks of focalized fractional radiotherapy alongside chemotherapy with an oral alkylating agent, such as temozolomide [4]. Since disease recurrence is eventually diagnosed in the majority of patients, re-irradiation has been reported to be an efficient retreatment option, whereas surgical reintervention is limited to selected cases [5, 6]. The addition of antiangiogenic immunotherapy [bevacizumab, a recombinant humanized monoclonal antibody (mAb)] gave promising results for the treatment of recurrent GBM [7]. Imaging has become an

integral part in every stage of glioma management, aiming to assess tumor response induced by multimodality treatment and manifested by changes in the anatomic and molecular level; it provides information that is critical to staging, formulating preoperative strategies, monitoring therapy response, postoperative surveillance and prognosis [8].

Anatomic imaging: Conventional contrast-enhanced MRI

Diagnosis of invasive brain lesions is made radiologically by revealing morphological alterations of the brain parenchyma. The method of choice is conventional (anatomic) magnetic resonance imaging (MRI) with intravenous (IV) gadolinium (Gd)-based contrast agent enhancement. Except in cases where MRI and/or gadolinium contrast is contraindicated, Gd-enhanced MRI is the typical procedure for the routine brain tumor imaging protocol in most institutions. The standard anatomic MRI sequences for diagnostic imaging of brain tumors typically include pre-contrast T1-weighted (T1w) and T2-weighted (T2w) spin echo, fluid-attenuated inversion recovery (FLAIR) and post-contrast T1w spin echo. Many protocols also routinely employ T2*w gradient echo. Far superior to computed tomography (CT), contrast-enhanced MRI provides essential anatomical information by excellent soft-tissue contrast, comparatively high resolution, compensating for the higher cost, and ready availability. It forms the basis upon which pre-surgical planning, post-operative assessment, radiotherapy planning, and post-treatment surveillance are accomplished [9].

Compared to the healthy brain, gliomas typically appear hypointense to myelinated white matter on T1w and hyperintense on T2w; they may also include hemorrhage and necrosis, while their boundaries are often ill-defined [8]. During the diagnostic process, it is decisive to differentiate brain tumors from benign lesions, such as demyelination, infarction, hematoma, and abscess, which may appear similar on MRI. Conventional MRI may face significant limitations in discriminating benign from malignant intracranial space-occupying pathology since this technique basically recognizes blood-brain barrier (BBB) disruption, mass-effects, and edema that can equally accompany neoplastic and non-neoplastic lesions. The MRI signal lacks biological specificity, e.g. T1w contrast enhancement reflects any non-specific increase in BBB permeability, while T2w signal abnormality is dominated by tissue water content (edema) [10]. Worth mentioning, many brain tumors –particularly WHO grade II and a substantial portion of grade III gliomas- do not enhance with contrast agent, reducing the ability of contrast imaging to accurately quantify tumor burden [11]. Hence, the low specificity of conventional MRI for neoplastic tissue is hampering the evaluation of tumor extent in both enhancing and non-enhancing gliomas. For that reason, advanced MRI techniques were developed in an effort to overcome these limitations concerning the discrimination of neoplastic from non-neoplastic lesions, which is of relevance in every phase of brain tumor management and particularly in the post-treatment setting.

Advanced MRI techniques

Although MR radiomorphology is useful for the detection and structural characterization of brain tumors, Gd-enhancement reflects BBB disruption rather than truly assesses tumor vascularity. Neovessels within brain tumors frequently lack a normal BBB, leading to an increase in vascular permeability. However, given that up to one-third of HGG do not exhibit gadolinium enhancement, the ability of Gd-enhanced MRI to distinguish between low- and high-grade tumors remains limited [11]. Conventional MRI cannot provide insight into a lesion's metabolism: it cannot reliably predict its malignant potential, glioma aggressiveness (low- or high-grade), while in treated gliomas it exhibits limited capability in diagnosing between treatment-related changes [pseudoprogression (usually occurring in the first 3 to 6 months after treatment) and radiation necrosis (from 9 months to years later)] and glioma recurrence (true progression) [12, 13].

To overcome these inherent limitations and provide physiologic information about gliomas that cannot be retrieved through standard anatomic MRI, several physiology-based advanced MRI techniques were developed in an attempt to delve beyond morphology into glioma biology. The ability to characterize tumoral and peritumoral tissue microstructure based on water diffusion and perfusion has provided clinicians with an entirely new perspective on improving glioma diagnosis and management. Perfusion-weighted and diffusion-weighted imaging (PWI, DWI) and MR spectroscopy (MRS) are the most widely used relevant modalities.

MR perfusion

Perfusion refers to the capillary blood supply of a tissue and MR perfusion enables the measurement of this microcirculation. Many brain tumors (especially HGG) exhibit neoangiogenesis that results in increased vessel density per unit volume of tissue, as compared to normal white matter and/or grey matter. This is observed by PWI as an increase in either the relative cerebral blood volume (rCBV) or the regional cerebral blood flow (rCBF) within the tumor [14]. Perfusion-weighted imaging is a contrast-enhanced MR perfusion technique to measure these tissue perfusion parameters within a lesion. The traversal of the Gd-based contrast agent through brain tissue can characterize vessel density because it creates a local magnetic field distortion in the vicinity of the vessels causing a signal drop in T2*w image (also called susceptibility effect, hence dynamic susceptibility contrast (DSC) T2*w imaging). It also leads to a shortening of T1-relaxation time, causing a signal increase in T1w image (also called dynamic contrast-enhanced (DCE) T1w imaging).

For assessing brain tissue perfusion following a rapid IV bolus injection of the paramagnetic contrast agent, DSC T2*w acquisition utilizes very fast imaging to capture the contrast first pass. The hemodynamic parameters that derive from DSC are the rCBV, rCBF and mean transit time (MTT). Relative cerebral blood volume reflects the amount of blood -and hence vessels-present in a given volume of tissue at a given time period. It can be estimated from the area under the fitted time-signal curve, whilst rCBF is computed by the ratio of rCBV to MTT [15]. Relative cerebral blood volume is the most commonly applied DSC-MRI metric for evaluating

brain tumors.

On the other hand, DCE T1w imaging requires longer acquisition time, because it is most often used in enhancing brain lesions with disrupted BBB to evaluate the continuous leakage of the contrast medium from the vascular compartment into the extravascular extracellular space (EES) by passive diffusion due to a concentration gradient. The hemodynamic parameters deriving from DCE are the vascular leakage constant (K^{trans}) and the efflux rate constant (k_{ep}). K^{trans} represents the forward influx volume transfer rate of the contrast medium from blood plasma to the EES and depends on blood flow, vascular surface area, and vascular permeability; k_{ep} is the corresponding reflux rate of the contrast medium from the EES back into plasma (Figure 1) [16]. T1w DCE images are typically higher resolution with fewer magnetic susceptibility artifacts than the T2*w DSC images [11].

Arterial spin labeling (ASL) is another promising PWI technique that, unlike DCS and DCE, it does not involve the administration of contrast agent [9]. Here, the endogenous water molecules in blood vessels are magnetically labeled by applying a specific radiofrequency pulse. Passing of these "labeled" molecules through a brain lesion leads to a reduction of signal intensity in proportion to the local perfusion. Arterial spin labelling allows perfusion assessment in cases of renal impairment, where gadolinium contrast is contraindicated. Quantification of flow with ASL is technically challenging because no contrast agent is used and thus the signal-to-noise ratio is inherently low, so repeated pulse scans are mandatory for signal averaging and this results in prolonged acquisition time.

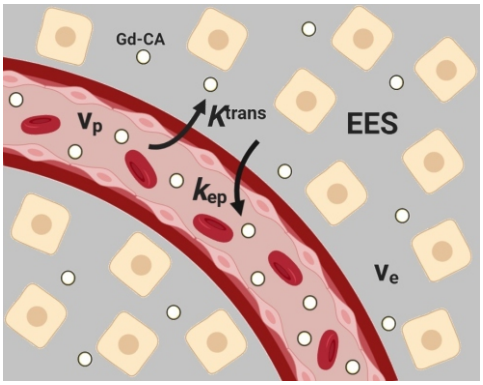

Figure 1. Pharmacokinetic principle of DCE MRI in brain lesions with BBB disruption (Tofts model [16]). The injected intravascular gadolinium-based contrast agent (Gd-CA) leaks through the vascular endothelium into the extravascular extracellular space (EES) at a constant rate (K^{trans}), without entering the cells. At the same time, it also leaks at another constant rate (k_{ep}) in the opposite direction, from EES back into the plasma; this bidirectional diffusion reaches an equilibrium. K^{trans}: forward (influx) transfer constant; k_{ep}: reverse (reflux) transfer constant; v_e: EES fraction volume (per unit volume of tissue); v_p: plasma fraction volume.

MR diffusion

Diffusion of water and other small molecules refers to their random, microscopic movement due to thermal collisions (Brownian motion). The technique called DWI does not require the administration of a contrast agent; it is rather based on the measurement of the Brownian motion of water molecules within the tissues and the degree to which their diffusivity is hindered by tumor cellularity [17]. By applying special diffusion-weighted gradients, the MR images are made sensitive to this motion. The degree of diffusion-weighting can be altered by variation of the pulse amplitude, duration and inter-pulse time, parameters determining the so-called b-value of the pulse. Diffusion-weighted imaging generates images based on the average water diffusivity in 3D space (X, Y, Z axes) within each voxel analyzed. The pulse sequence is first run with the gradient turned off (b=0) to produce a T2w image that serves as a baseline for later calculated maps. Then two opposing gradient pulses (b>0) are acquired: the first induces a phase shift in water molecules, leading to a signal reduction, and the second (opposed) pulse rephases the water molecules and leads to recovery of the water signal, thus producing source images sensitized to water diffusion in multiple different directions (X, Y, Z). By combining these source images, a trace (geometrical mean) image of diffusion is produced. The baseline image and trace images of at least two different pulse b-values are needed to calculate the apparent diffusion coefficient (ADC) for each voxel. The resulting ADC image -also referred to as the ADC map- depicts a quantitative measure of water diffusivity in every region of the brain [18].

Calculated ADC maps represent a means of displaying information about the apparent diffusion of water molecules without the T1- and T2-relaxivity effects inherent in the diffusion-weighted images themselves [17]. Increased cellular density in malignant brain tumors leads to restriction of water diffusivity and lower ADC signal values [19]. However, meningiomas, as well as non-neoplastic central nervous system (CNS) lesions (e.g. acute infarcts, pyogenic abscesses), may exhibit similarly low ADC values [20, 21]. Nevertheless, ADC histogram analysis has been shown to carry prognostic information in both newly-diagnosed and recurrent GBM treated with antiangiogenic therapy [22, 23].

Diffusion tensor imaging (DTI) is another MRI technique that enables the measurement of restricted water diffusion in brain tissue. Water diffusivity can be either isotropic (i.e. unrestricted), when there are no hinders to diffusion, being statistically the same in every direction (X, Y, Z) (e.g. in the cerebrospinal fluid); and anisotropic, when diffusion encounters barriers in certain directions (e.g., in the axons forming the white matter). The architecture of axons in parallel bundles and their myelin shield facilitate longitudinal water diffusion along their main direction rather than perpendicularly (Figure 2). Diffusion tensor imaging acquires water diffusion information by applying a minimum of six diffusion-sensitizing gradients with different orientations and calculates, for each voxel, a tensor math that describes this diffusion anisotropy. In the generated parametric image (map) of fractional anisotropy (FA), each voxel has one or more pairs of parameters: a rate of water diffusion and a preferred directionality of diffusion in 3D space. Beyond plain diffusivity, FA incorporates the degree of directionality, in that a voxel with FA of zero indicates isotropic water diffusion in all directions, whereas an FA of one indicates a restriction of diffusion to a single axis of motion [24]. Hence the generated FA map reflects on fiber directionality and densi-

ty, axonal diameter and white matter myelination. This directional information can also be exploited to depict neuronal tracts through the brain, a process called fiber tracking or tractography. Diffusion tensor imaging delineates the margins of primary brain tumors better than anatomical MRI [25]. It has been shown to differentiate between LGG and HGG and to distinguish between GBM and metastases, while tractography improves surgical safety by guiding neurosurgical planning and allowing greater tumor resection [26-28]. Figure 3 describes a demonstrative paradigm of the added diagnostic value provided by advanced diffusion and perfusion MR techniques in the management of glioma.

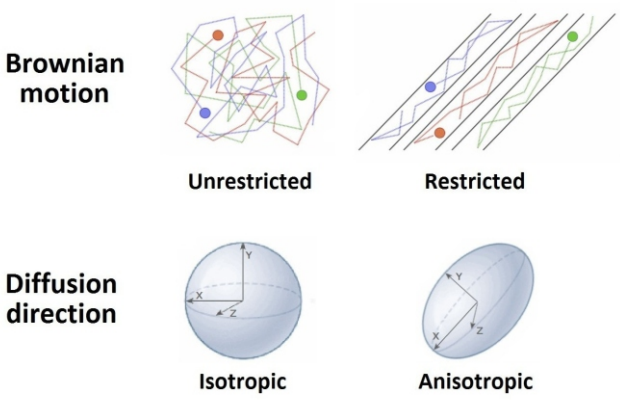

Figure 2. Schematic representation of the diffusor tensor MRI working principle.

MR spectroscopy

Proton MRS is a method to detect selected water-soluble metabolites in vivo using either data from a single voxel or multiple voxels in a single slice or multiple slices of a brain lesion. Every tissue metabolite molecule has its characteristic magnetic field "signature". Combined with interactions amongst the nuclei, these results in slightly different resonance frequencies leading to differential signals. MRS uses these spectral signal differences to identify various metabolites within brain lesions. Although no tumor-specific metabolite has been identified to date, the main metabolites of interest for brain tumor characterization include N-acetyl aspartate (NAA), a marker of neuronal integrity; choline (Cho), a marker of cellular membrane synthesis; lactate (Lac), a product of anaerobic glycolysis; lipids (Lip), byproducts of necrosis; creatine (Cr), a marker of bioenergy storage; glutamate-glutamine (Glx), a neurotransmitter; myo-inositol (mI), a glial cell marker; and alanine (Ala), a meningioma cell marker [29].

By recognizing characteristic changes in the metabolite profile within a brain lesion, as compared to the normal brain parenchyma, MRS provides important diagnostic biochemical information that is not obtainable through conventional anatomic MRI [30]. The technique has been evaluated for the differentiation of neoplastic from non-neoplastic CNS lesions (such as brain abscess, demyelination, infarct, and radiation necrosis) with good results. Elevation of Cho due to increased cellular membrane synthesis is the hallmark of an actively growing malignant brain neoplasm, along with a decrease in NAA due to neuronal loss in a primary brain tumor, or a lack of NAA in metastasis [29]. Lac is interpreted as a marker for hypoxia and the presence of Lip indicates tumor necrosis; both these metabolites also represent additional features of malignancy. As the grade of glioma malignancy increases, the metabolic peaks of NAA and Cr decrease, whereas Cho, Lip and Lac peaks increase (Figure 4) [31, 32]. The presence of mI is a marker for glial cell lineage, while certain other metabolites may be indicative of specific tumor types (e.g., Ala in meningiomas) [29]. The absolute quantification of CNS metabolites using MRS remains challenging in the clinical environment and therefore semi-quantitative assessments of MR spectra using metabolite ratios are often used in clinical practice. A marked elevation of the Cho/NAA and Cho/Cr ratios is therefore considered a sign of malignancy [9].

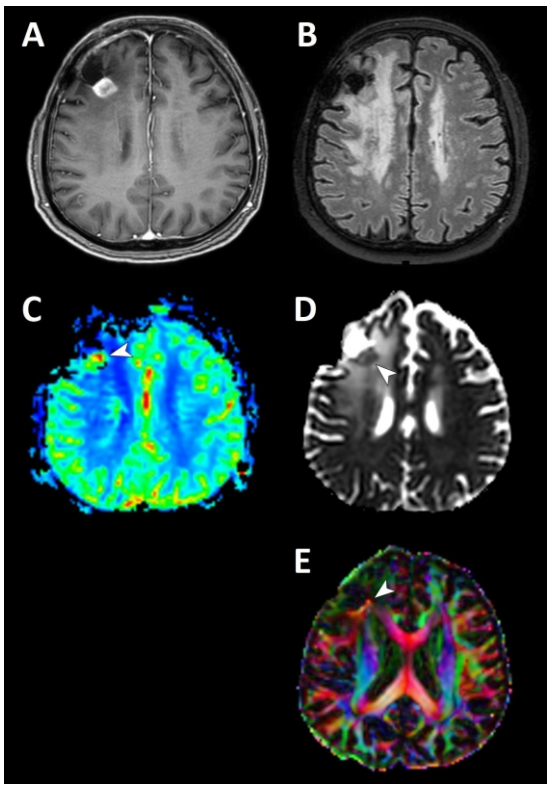

Figure 3. A 66-year-old male, diagnosed two years earlier with GBM of the right frontal lobe and treated by surgery and radiochemotherapy, was re-evaluated due to clinical deterioration. **A)** Gd-enhanced T1w MRI showed a post-surgical cavity with an adjacent enhancing dense area that raised the question of tumor recurrence versus radiation necrosis. **B)** FLAIR imaging showed white matter edema, not only in the corresponding brain hemisphere but also contralaterally. **C)** Further investigation by DSC revealed increased rCBV *(arrowhead)* in the corresponding area of Gd-enhancement, indicating intense angiogenesis. **D)** Within the extensive surrounding edema, the DWI ADC map pointed at an area of focally decreased values *(arrowhead)*, suggesting a hypercellular lesion with restricted water diffusivity. **E)** DTI with FA color mapping revealed disruption predominantly of the association white matter fibers *(arrowhead)* in the corresponding area. Shortly after a new surgery verified tumor recurrence.

Single-voxel spectroscopy is the most widely used technique due to simple data acquisition and short scanning time, yiel-

ding high signal-to-noise ratio and high-quality spectra that enable straightforward interpretation. However, manual region-of-interest (ROI) selection based on structural information from T2w or Gd-enhanced T1w sequences may represent only a fraction of the tumor, potentially resulting in an incomplete evaluation of tumor biology. This limitation can be overcome by multi-voxel techniques that cover a more extended 2D or 3D ROI, which is particularly useful in heterogeneous lesions [33]. However, because of the difficulty to attain good shimming over a large enough region, multi-voxel spectroscopy may achieve a lower signal-to-noise ratio, requires longer scanning times and is technically more demanding [34]. Acquisition of a good metabolic peak is negatively affected by such problems as chemical shift artifacts, insufficient water suppression, or inadequate shimming. In practice, MRS is highly operator-dependent in that an ROI must be selected to avoid areas of necrosis, hemorrhage, calcification, or tumoral cysts and then carefully shimmed in order to obtain interpretable MR spectra. Combining MRS with images from other advanced techniques, such as rCBV and ADC maps, is reported to improve diagnostic accuracy [35].

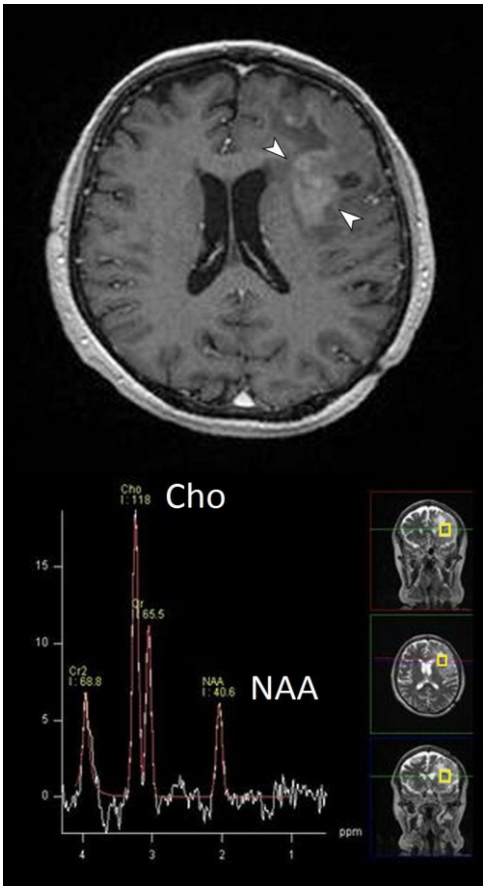

Figure 4. Newly-diagnosed HGG of the left frontal lobe with only marginal contrast enhancement (arrowheads). MRS depicted increased Cho and decreased NAA peaks, a peak reversal pattern that is highly suggestive of malignancy.

Metabolic PET imaging

To gain additional diagnostic information from that acquired by conventional MRI and advanced MRI techniques, nuclear medicine metabolic imaging has been employed towards the evaluation of brain tumors. This involves IV injection of radioactively labeled tracer probes to target various metabolic and molecular pathways, aiming to provide insight into the pathophysiology and metabolism of glioma. These metabolic imaging techniques comprise single-photon emission tomography (SPET) and positron emission tomography (PET). The primary role of molecular imaging pertains to the non-invasive assessment of tumor grading and aggressiveness, differentiation between non-specific treatment-related changes from tumor progression and recurrence, assessment of glioma response to treatment and estimation of patient prognosis.

Single-photon emission tomography offered a credible functional imaging modality with the relative advantages of lower cost and wider availability [36]. However, it is PET that may be credited with providing the impetus for the clinical interest in molecular neuroimaging. It has better spatial resolution than SPET, its combination with simultaneous radiomorphological imaging (PET/CT & PET/MRI integrated systems) is an established industry standard for all modern PET cameras and it has great potential for the development of novel radiotracers, thus contributing important information especially in clinically challenging situations to improve diagnosis, therapy planning, and post-treatment surveillance.

Several PET tracers exhibiting various oncophilic properties have been used for metabolic imaging of gliomas. Their shared feature is that they mimic (or are sometimes chemically identical to) metabolites that are avidly taken up and retained by proliferative tumor cells. These include sugars [fluorine-18 [^{18}F]-fluoro-2-deoxy-D-glucose (FDG)]; amino acids [carbon-11 [^{11}C]-methyl-L-methionine (MET), ^{18}F-fluoroethyl-L-tyrosine (FET), ^{18}F-fluoro-L-phenylalanine (FDOPA)]; pyrimidine bases [^{11}C-thymidine, ^{18}F-fluoro-L-thymidine (FLT)]; phospholipid precursor molecules of the vitamin B complex [^{11}C-choline (CHO), ^{18}F-fluoro-choline (FCHO)]; and nitroimidazoles [^{18}F-fluoromisonidazole (FMISO), ^{18}F-fluoroazomycin arabinoside (FAZA)]. Positron emission tomography imaging offers the unique potential of depicting metabolic information about brain tumor biology that is not attainable through anatomic imaging, hence the incremental diagnostic yield of imaging pathophysiologic glioma processes like glucose metabolism, amino acid transport, cellular proliferation, membrane synthesis, and hypoxia is under meticulous systematic investigation [9].

Glucose analog: ^{18}F-FDG

Fluorine-18-FDG is the most extensively used PET tracer to date, due to its exceptional importance in general oncology. It is an analog for glucose and thus a tracer for brain energy metabolism, resulting in reduced contrast between tumor and normal cerebral tissue. For that reason, its applicability in brain tumor diagnostics is hindered by the high levels of physiological glucose uptake in the cerebral cortex. Fluorine-18-FDG exploits the upregulation of glycolysis in cancer cells and accumulates intracellularly through the glucose transporter (typically GLUT-1), where it is phospho-

rylated by hexokinase. The fluorine atom precludes further metabolism through the normal glycolytic cycle, so ^{18}F-FDG is trapped in the cell and not further catabolized [37].

Certain gliomas are known to overexpress hexokinase and therefore in these tumors, ^{18}F-FDG PET may overestimate glucose consumption [38]. Identification of brain tumor tissue by ^{18}F-FDG uptake is usually made by qualitative comparison to the grey matter and/or white matter uptake. In LGG, ^{18}F-FDG uptake is typically similar to that in normal white matter, while in HGG it is variable, but often similar to that in normal grey matter. To overcome these inherent restraints and improve discrimination between tumor and normal background uptake, delayed imaging has been proposed on the basis of prolonged tumoral retention of ^{18}F-FDG relative to normal grey matter [39]. Fluorine-18-FDG uptake ratios of tumor-to-normal white matter and tumor-to-normal grey matter have been used for distinguishing between LGG and HGG [40]. However, certain LGG (e.g., pilocytic astrocytoma, ganglioglioma) exhibit relatively high ^{18}F-FDG uptake despite their low grade; on the other hand, uptake in high-grade tumors can be less than, or similar to that of normal gray matter and GBM with necrosis often appears as a prominently heterogeneous lesion with adjacent areas of high and low tracer uptake [9, 40]. In spite of these limitations, ^{18}F-FDG uptake in gliomas was shown to correlate with both tumor grade and survival [41].

Although distinguishing metabolically active tumor from delayed radionecrosis in the post-treatment setting is one of the most common clinical indications for PET imaging in brain tumors, ^{18}F-FDG PET exhibits moderate diagnostic accuracy in differentiating tumor recurrence from treatment-related effects, regardless of whether white matter or grey matter is used as the internal reference standard. Apart from physiologic cerebral ^{18}F-FDG uptake, other reasons for this include elevated glucose metabolism by the treatment-induced immune cell activation within areas of inflammatory response and apoptosis [42, 43].

Amino acids & analogs: ^{11}C-MET, ^{18}F-FET, ^{18}F-FDOPA

Amino acids present several advantages over ^{18}F-FDG and other PET tracers and are now regarded as the tracers of choice for PET imaging of brain tumors (Figure 5) [44, 45]. To provide the essential amino acids needed for brain protein synthesis, amino acid transporters are expressed in normal brain tissue cells as well as in the BBB. L-type amino acid transporters 1 and 2 (LAT1 and LAT2) facilitate the diffusion of neutral amino acids across cellular membranes. The tissue uptake of commonly used PET amino acid radiotracers is largely dependent on these Na^+-independent transporters. In glioma cells, the expression of amino acid transporters is upregulated in correspondence to their increased metabolic needs. Studies using labeled amino acid analogs that are not incorporated into protein synthesis revealed that increased tracer uptake in gliomas is mainly driven by augmented amino acid transport rather than by protein synthesis *per se* [46]. The principal advantage of amino acid tracers is that their uptake is independent of the BBB integrity; compromise of the BBB by tumor growth is not a requisite for amino acid tracer permeability, thus allowing evaluation of non-enhancing gliomas (usually LGG) with uninterrupted BBB, which may infiltrate in the seemingly intact surrounding brain and already be transforming into a higher grade [13, 19]. Furthermore, their uptake is relatively low in normal cerebral tissue whereas it is typically increased in brain tumors, thus resulting in an easily perceptible enhanced tumor-to-background contrast [44, 47].

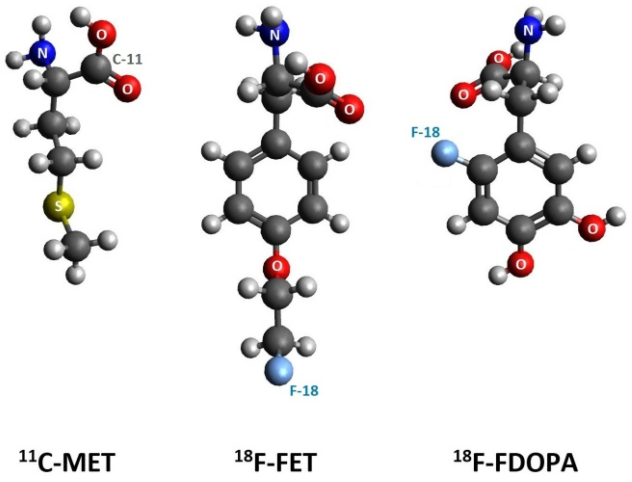

Figure 5. Molecular structure (3D conformer) of the most widely used amino acid PET tracers [45].

Among the amino acid tracers used in neuro-oncological PET, ^{11}C-MET is one of the most widely applied and best evaluated [48]. However, its use is restricted to centers with an on-site cyclotron owing to the short half-life (20min) of ^{11}C. To overcome this logistical limitation, labeling with ^{18}F (with a longer half-life of 110min) allowed the development of a number of readily available amino acid tracers. Hence ^{18}F-FET has become the most widely used radiotracer in many neuro-oncological centers and largely replaced ^{11}C-MET in brain tumor diagnostics [19]. It must be noted, however, that the slower renal elimination rate of ^{18}F-FET from the blood pool may result in prolonged nonspecific tracer retention in the cerebral venous sinuses and in vascular malformations, which might impose differentiation challenge from a metabolically active tumor [44]. Fluorine-18-FDOPA was originally developed as a radiotracer for imaging of the DOPA-decarboxylase pathway in parkinsonian neurodegenerative disorders, but it has also been studied as a marker for L-amino acid transport in brain tumors. Although gliomas distant to the striatum are depicted with high contrast, the preferential striatal uptake of ^{18}F-FDOPA raises an obstacle in the accurate delineation of tumors located in the basal ganglia area [49].

Pyrimidine bases: ^{11}C-thymidine, ^{18}F-FLT

In addition to ^{18}F-FDG and radiolabeled amino acids, several other PET probes have been applied in brain tumor imaging. Thymidine is a native pyrimidine base used in DNA synthesis, thus ^{11}C-thymidine PET has been considered as a potential imaging biomarker for identification of active DNA

synthesis and tumor proliferation. Thymidine is a substrate for thymidine kinase-1 (TK-1), the principal enzyme in the pathway of DNA synthesis, but is also a substrate for mitochondrial TK-2 and this limits its specificity as a potential marker for active cell division. Furthermore, radiolabeled thymidine suffers from rapid in vivo degradation into several metabolites and the limited availability issues of the short-lived ^{11}C [38].

For these reasons, the thymidine nucleoside analog ^{18}F-FLT has been developed as an alternative estimator of DNA synthesis and cellular proliferation. Fluorine-18-FLT enters the cell through the cell membrane by facilitated diffusion; there, it is phosphorylated by TK-1 and not further metabolized, resulting in intracellular trapping in a manner analogous to ^{18}F-FDG trapping by hexokinase [50]. Dissimilar to thymidine, ^{18}F-FLT is a poor substrate for TK-2; its uptake reflects the specific to the cell cycle TK-1 activity and hence it may provide a quantitative measure of cellular mitotic activity [51]. During DNA synthesis the TK-1 increases tenfold, so actively proliferative glioma cells take up ^{18}F-FLT to a significantly higher degree compared to the normal brain parenchyma. Dissimilar to ^{18}F-FDG, ^{18}F-FLT does not accumulate in inflammatory lesions; activated immune cells primarily undergo aerobic glycolysis and, therefore, are not detected by ^{18}F-FLT, which is thus suitable to depict cellular proliferation [8]. However, unlike labeled amino acids, the intact BBB is impermeable to ^{18}F-FLT and this obviously precludes its clinical usefulness in non-enhancing lesions (Figure 6) [52, 53]. But even in contrast-enhancing gliomas, ^{18}F-FLT uptake is governed also by its transport rate across the ruptured BBB and not solely by DNA synthesis (TK-1 activity), so any assumption that ^{18}F-FLT uptake in glioma reflects exclusively cellular proliferative activity is potentially misleading [54].

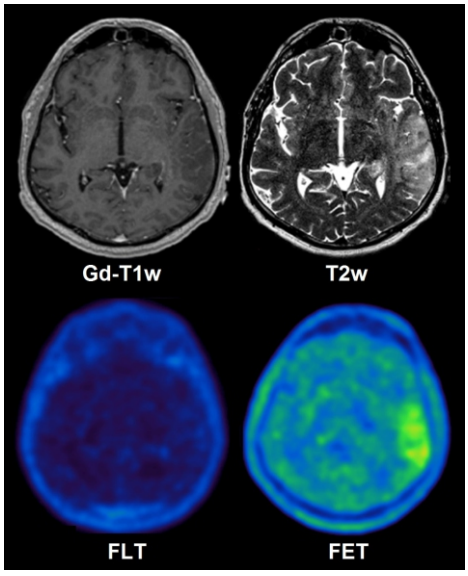

Figure 6. Newly-diagnosed left parieto-temporal GBM presenting as a hyperintense lesion on T2w but without contrast enhancement on Gd-T1w. Contrary to the absence of ^{18}F-FLT uptake, a metabolically active lesion is clearly depicted on ^{18}F-FET PET. Reproduced under a Creative Commons Attribution License CC BY 4.0 from copyright holders Martha Nowosielski and colleagues; PLoS One, published by PLOS ONE, San Francisco, USA, and Cambridge, UK, 2014 [53] / Image relabeled from the original.

Phospholipid precursors (Vitamin B complex): ^{11}C-CHO, ^{18}F-FCHO

Increased choline uptake by tumor cells can be attributed to an intensified demand for membrane constituents. The concept of assessing cellular membrane turnover bears obvious similarities with that of assessing protein synthesis by amino acid tracers and DNA synthesis by pyrimidine base tracers. Choline is a phospholipid precursor entering the cell by means of specific transporter activity and, once inside the cell, is phosphorylated by the enzyme choline kinase. Subsequently, it takes part in the cell membrane synthesis by integration into phosphatidylcholine (lecithin), an essential constituent of phospholipid membranes [55]. It is already clear for amino acids that transport, not metabolism, is the critical issue governing tracer uptake and this also seems to be the case for choline radiotracers.

Choline can be labeled either by ^{11}C (^{11}C-CHO) or ^{18}F (^{18}F-FCHO). Tracer uptake in gliomas seems highly related to transport and choline kinase activity of the tumor cells themselves but is also influenced by tumor microvessel density and the BBB [specific transport (more likely) or disruption] [56, 57]. Initial results of radiolabeled choline clinical application come from small studies and heterogeneous populations; these support the use of choline tracers in the management of glioma, though larger studies are needed for better validation.

Nitroimidazoles: ^{18}F-FMISO, ^{18}F-FAZA

Tumor hypoxia is an important clinical factor because it is associated with malignant progression and resistance to the effects of radiotherapy. Conventional radiotherapy depends upon the availability of oxygen to form free radicals that result in DNA damage and thereby induce cancer cell apoptosis. The radiotracer ^{18}F-FMISO has been widely used for imaging hypoxia in brain tumors, while ^{18}F-FAZA provides an attractive alternative [58]. Nitroimidazoles cross freely the intact BBB and the cellular membrane by passive diffusion and are enzymatically reduced by cellular nitroreductases and trapped inside viable glioma cells only under severely hypoxic conditions and not within necrotic tumor areas. Tumor hypoxia defined by ^{18}F-FMISO PET has been observed more often in HGG than in LGG and correlates with shorter survival [59]. Although ^{18}F-FMISO is of interest and promising results have been reported for identifying hypoxic tumor areas, it is not yet clear whether guidance of external beam radiotherapy based on PET findings may lead to better therapeutic outcomes, since to date the method has predominantly been used in a preclinical setting [60].

Correlative glioma imaging with amino acid PET and advanced MRI techniques

Over the past few decades, advanced MRI techniques are being evaluated in the clinical setting and they provide complementary (patho)physiological information to that obtained by standard MRI. At the same time, owing to their advantageous imaging characteristics, radiolabeled amino acids have evolved into a significant diagnostic tool up ahead of ^{18}F-FDG and other PET tracers. As a result, recent joint

recommendations of the Response Assessment in Neuro-Oncology working group (RANO) and the European Association for Neuro-Oncology (EANO) consider amino acid PET as clinically helpful in the management of patients with brain tumors and propose its use additionally to classic MRI at every stage of disease [61].

The most significant experience of correlative imaging between multimodal MR and PET in gliomas originates from medical centers that have access to both modalities and apply them on a daily basis in brain tumor workup. The vast majority of this experience pertains to the reference standard of amino acid PET (for obvious reasons), which is compared mostly with rCBV, due to its superior diagnostic performance as against other advanced MRI parameters for glioma monitoring [62, 63]. The performance of PET and advanced MRI is principally examined in the clinical settings of differentiating between malignant and non-malignant brain lesions; in tumor grading (low- vs. high-grade); in establishing patient prognosis; in delineating tumor extent; in guiding stereotactic biopsy; in monitoring tumor response to treatment (and identifying pseudoresponse); and in discriminating early tumor progression or late recurrence from treatment-related brain changes (i.e., pseudoprogression and radiation-induced necrosis, respectively).

When a brain lesion of unclear origin is diagnosed, it is of paramount importance to differentiate between glioma and a non-neoplastic lesion. Labeled amino acids generally show higher uptake in neoplastic pathologies and increased uptake in benign lesions is rare. However, false-positive uptake has been reported in abscesses, demyelinating lesions, ischemic strokes and hemorrhages [64]. Comparative studies between amino acid PET and PWI are not readily available. In a head-to-head study involving ^{18}F-FET PET and single-voxel MRS (NAA/Cho ratio) in a series of 50 newly-diagnosed intracranial lesions, there was significant congruence between the two modalities in identifying glioma (88% and 94% diagnostic accuracy, respectively) [65]. Both PET and advanced MRI may contribute usable additional information for the characterization of equivocal CNS lesions, but still, there is a need for additional studies.

Histopathology is the reference standard for tumor grading and pivotal for treatment planning and prognostication. However, sometimes tissue samples are not obtained from the most aggressive part of the tumor, whilst occasional varying interpretations by different neuropathologists may rise diagnostic uncertainties. In such cases, the agreement between histopathology and non-invasive imaging parameters may reinforce clinical decision-making. A review of the studies assessing amino acid PET in differentiating between LGG and HGG indicates that the modality does not allow for a reliable prediction of tumor grade, due to the highly variable tracer uptake resulting in overlap between different WHO grades; the measured diagnostic accuracy was moderate, in the range of 70%-80%, comparable to that of ^{18}F-FDG PET and PWI [66, 67]. Despite the better prognosis of OD from same-grade AS, the OD component exhibits increased amino acid turnover compared to AS [68]. Dynamic ^{18}F-FET PET with kinetic tracer analysis may to some extent improve the discrimination between HGG and LGG: time-activity curves of grade II tumors exhibit a slow, steady increase, compared to the rapid uptake by grade III/IV tumors [69, 70]. The significance of PWI for tumor grading has also been investigated in numerous studies with varying results [71-73]. Although LGG generally display low rCBV, the presence of an OD component may be associated with elevated rCBV, analogous to their increased amino acid uptake in PET [74]. Therefore, although amino acid PET and PWI may provide some noninvasive clues on glioma grading, they cannot currently supersede the diagnostic significance of histopathology.

As regards the prediction of patient outcome and prognosis, amino acid PET seems to be useful in predicting survival in LGG [75, 76]. Recent studies also indicate that the metabolic tumor volume of HGG represents an independent factor of prognostic significance [77]. Fluorine-18-FET uptake reduction following radiochemotherapy was associated with favorable overall survival compared to stable or increased uptake [78]. Correspondingly, PWI studies reported a correlation of increasing glioma rCBV with worse overall survival [79, 80]. Further research is required to gain a clearer insight into the potential role of each imaging modality in glioma prognostication.

The recently revised WHO glioma classification scheme recognized molecular biomarkers as an important concept in prognostication and survival, with IDH mutation and 1p/19q co-deletion being key factors [3]. Thenceforth, a series of studies assessed amino acid tracers as potential biomarkers of molecular status; any reported significant correlations, however, are not yet sufficient to permit a noninvasive prediction of glioma molecular profile based on PET data alone and further multicenter studies are required to endorse potential clinical merit [67].

At diagnosis of cerebral glioma, the depiction of the true extent of the tumor and biopsy guidance is of vital importance for the correct histological diagnosis and grading, evaluation of molecular status (IDH, 1p/19q), prognostication and treatment decisions. Classic MRI faces inherent inadequacy in that area and may result in underdiagnosis, particularly in non-enhancing lesions. Amino acid PET is clearly advantageous over standard MRI in delineating tumor extent and this has been used in numerous studies for planning surgical resection and radiation therapy [81-83]. Studies that investigated the diagnostic value of PWI or DWI in this indication reported contradictory results concerning the spatial congruency between amino acid uptake and rCBV or ADC abnormalities [84-87]. These study results concerning spatial incongruences are most likely related to the fact that amino acid PET and PWI/DWI encode different biological processes. Furthermore, the interpretation of rCBV and ADC maps is more challenging than the evaluation of cerebral amino acid uptake. At the same time, factors such as tissue compression and ischemia may be contributing to restricted diffusion and result in a poor correlation between sites of minimal ADC and increased amino acid uptake [85]. Hence PET appears to be more reliable for detecting the extent of gliomas. Regarding MRS, a comparative study involving 2D multi-voxel imaging and ^{18}F-FET PET found significant correlations between increased tracer uptake and the extent of neuronal loss (NAA) and partially with

membrane synthesis (Cho) [88]. However, in another recent 3D MRS study the ^{18}F-FET uptake and increased Cho/NAA ratios were not consistently spatially congruent, indicating the need for further investigation [89].

With reference to the identification of the most aggressive tumor area to guide tissue sampling, both modalities have been used to target the most malignant location of gliomas. Amino acid PET has been shown to be very sensitive in identifying metabolic hot spots [90, 91]. Some head-to-head studies reported spatial correspondence of the most active tumor loci, while others found considerable incongruences between PET and PWI [49, 92-94]. Both methods can be helpful for image-guided stereotactic biopsy, but further comparative studies are needed to elucidate whether amino acid uptake or rCBV corresponds better to the most aggressive part of gliomas.

Establishing glioma diagnosis through surgical excision or by biopsy is typically followed by a course of radiotherapy, chemotherapy (temozolomide), or antiangiogenic immunotherapy (bevacizumab) in the case of tumor recurrence. Effective treatment monitoring for early recognition of tumor response is of paramount importance for the optimization of individual treatment planning. The detection of viable tumor despite ongoing therapy, or tumor recurrence after therapy completion, addresses a crucial clinical question and often results in either a modification of the treatment plan or a change to a different therapy. The reliability of amino acid PET to stratify tumor response to treatment and to predict progression-free survival was shown by several studies and arises since as early as a week after GBM treatment completion, to several months earlier than MRI response of LGG [78, 95, 96]. Despite more widespread availability to PET, a few studies have evaluated the performance of PWI in early treatment assessment and further comparative investigations are needed.

Radiolabeled amino acids can effectively address another problem specific to antiangiogenic immunotherapy called tumor pseudoresponse; this occurs within days of initiation of treatment and is characterized by a rapid decrease in contrast enhancement on MRI or CT, despite the underlying growth of the non-enhancing portion of the tumor. Rather than a true antitumor effect, this phenomenon is partly attributable to the normalization of leaky tumor blood vessels, resulting in BBB restoration and reduced vascular permeability to contrast agents. The diagnostic accuracy of conventional MRI in this clinical setting is inherently low; on the contrary, delineation of a metabolically active tumor even after vascular normalization by bevacizumab, signifying treatment failure, can be detected accurately by amino acid PET as early as two weeks after therapy initiation [97, 98].

In the era of combined radiochemotherapy for initial treatment of newly-diagnosed HGG, the need for reliable discrimination between treatment-induced brain injury and tumor progression or tumor recurrence has become increasingly imperative in the clinical setting of patient follow-up. According to the time of appearance, treatment-induced changes mainly take the form of subacute-phase pseudoprogression (first 3 to 6 months), or delayed-phase radiation necrosis (9 months to years later). Both entities are characterized by an increase of contrast enhancement that is indistinguishable from true tumor progression on conventional MRI. Pseudoprogression pertains to a transient increase in the size of Gd-enhancement, or the appearance of new enhancement and usually occurs within the first 12 weeks after radiotherapy in up to 20%-30% of patients with HGG treated with concomitant temozolomide. These lesions decrease in size or stabilize without additional treatment and often remain clinically asymptomatic. Additionally, there is evidence that treatment-induced radiation necrosis occurs more frequently and earlier (6-9 months) after combined radiochemotherapy than after radiotherapy alone [99].

Fluorine-18-FET PET has been found with excellent diagnostic accuracy of 96% in discriminating pseudoprogression from true early GBM progression in the subacute phase of post-treatment follow-up [100]. Perfusion-weighted MRI studies involving both DSC and DCE for assessing pseudoprogression are more abundant and their diagnostic performance is satisfactory, though not as remarkable as PET, probably because rCBV is influenced by BBB disruption [101, 102]. More data are available on the performance of the two imaging modalities during the delayed phase of differentiation between tumor recurrence and radionecrosis. Amino acid PET performs equally well in this setting; in the majority of studies involving all available radiotracers (^{18}F-FET, ^{18}F-FDOPA, ^{11}C-MET), the diagnostic accuracy ranged between 82% and 93% (Figure 7) [103-105].

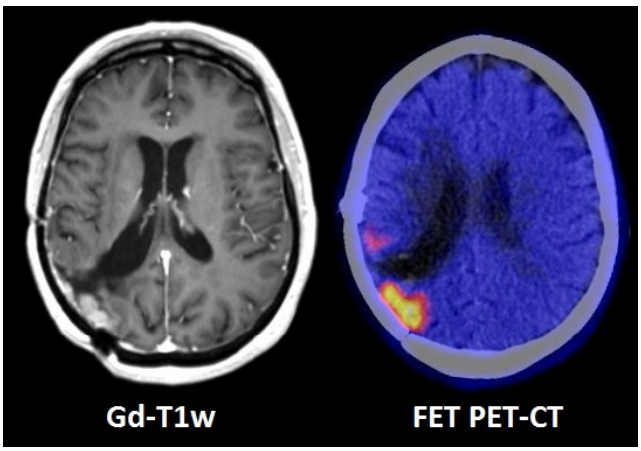

Figure 7. A 59-year-old female with a diagnosis of right parietal HGG was reevaluated two years after initial treatment, due to possible recurrence. Gd-enhanced T1w MRI showed an enhancing lesion in the area of previous surgery. Fluorine-18-FET PET/CT unveiled increased metabolic activity in the corresponding enhancing lesion, indicating tumor recurrence. Of note, an adjacent second focus of tracer uptake corresponds to a cortical area non-enhancing on Gd-T1w. Images courtesy of Drs. Vasileios Prasopoulos and Theodoros Pipikos, Department of PET/CT, *Hygeia* Hospital, Athens, Greece.

The performance of DSC and DCE to correctly classify late treatment-related changes were assessed in several studies, resulting in cumulated sensitivity and specificity of 90% and 88%, respectively [102]. Some studies have compared amino acid PET with PWI and reported on a similar diagnostic power [104, 106, 107]. A comparison between MRS or DWI and amino

acid PET in recurrent glioma was addressed in a few small-scale studies with promising results. Cho/Cr ratio metrics deriving from single-voxel MRS versus ^{11}C-MET uptake for the detection of recurrent HGG found a comparable diagnostic accuracy of 86% and 90%, respectively [104]. A significant spatial correspondence has also been described between minimal ADC values and increased ^{18}F-FDOPA uptake in recurrent HGG [108]; still, another study in HGG reported a superior performance for ^{18}F-FET PET compared to ADC [109]. In summary, current literature evidence suggests that both modalities provide particularly helpful diagnostic aid for differentiating actively metabolic glioma tissue from confounding treatment-induced changes, namely true tumor progression from pseudoprogression in the subacute phase and tumor recurrence from radiation-induced necrosis in the delayed phase after treatment.

Integrated PET/MRI in the management of glioma

Combined PET/MRI was proposed for imaging patients in the mid-2000s; since then, substantial progress has been made in technical versatility and methodological implementation in clinical practice. By merging the high spatial resolution and soft tissue characterization of Gd-enhanced MRI with the physiologic and metabolic information attainable by PET and advanced MRI techniques, simultaneous acquisition of MRI and PET allows for the direct correlation between different imaging parameters within the same imaging session. The patient retains the same position during both examinations and co-registration of the images is performed on-site, which greatly reduces mismatches between the two modalities and improves diagnostic specificity [110].

Early PET/MRI research in gliomas focused on the comparison between the two modalities in guiding stereotactic brain biopsy. In a series of diffusely infiltrating non-enhancing gliomas, MRS exhibited considerable overlap with ^{11}C-MET uptake in revealing anaplastic areas for surgical tissue sampling [111]. In another ^{18}F-FET PET/MRI series comprising both LGG and HGG, tracer uptake and increased Cho/NAA ratio were not always congruent, implying that they may represent different properties of glioma metabolism [112]. In a variety of HGG and LGG, increased cellular proliferation assessed by increased ^{18}F-FLT uptake and multimodal MRI (low ADC, increased Cho) identified similar areas for targeted biopsy with MRI markers of high vascularity (increased rCBV, DCE, ASL) [113]. Yielding all necessary information in one examination session with reduced radiation exposure (compared to PET/CT) is of major importance for oncological PET/MRI applications in the pediatric population and this applies also for stereotactic neuronavigation, for preoperative planning and predicting response to therapy [114, 115].

High spatial conformity of PET and MRI in the combined PET/MRI setting has been reported to benefit radiotherapy treatment planning both at initial therapy and on re-irradiation after recurrence [116, 117]. In the post-treatment setting, combined ^{11}C-MET PET/MRI was highly accurate in detecting glioma recurrence and it enhanced diagnostic confidence [118]. Further work in the evaluation of brain tumors with PET/MRI is anticipated to provide additional correlations between advanced MRI parameters and PET metabolic parameters, aiming to integrate multimodality PET/MRI information in improving preoperative diagnosis, optimizing surgical outcomes, enabling individualized treatment and facilitating post-treatment assessment [9].

In conclusion, classic anatomic contrast-enhanced MRI is of paramount importance in identifying structural brain abnormalities related to the development of space-occupying lesions, especially when those pathologies disrupt the BBB. It remains the current standard of care for glioma initial diagnostic workup, surgical planning, post-therapy response assessment, and follow-up surveillance. Nevertheless, the true nature of each lesion lies beyond the often misleading gross structural patterns, down to the cellular and molecular level. This is where advanced multimodal MRI techniques and metabolic PET imaging come into play. Out of the numerous tumor-seeking PET tracers available to date, radiolabeled amino acids have been proven highly relevant for brain tumor imaging; being able to penetrate lesions regardless of their BBB status, amino acid uptake translates into precise tumor boundary delineation and early treatment response assessment that rises above the classic MRI-related limitations of pseudoresponse and pseudoprogression (Figure 8) [8]. For that reason, they are currently considered as the reference PET standard and their increasingly upgraded role in patient care has been acknowledged recently by the integration of metabolic amino acid imaging in the updated RANO/EANO clinical recommendations for glioma management.

Positron emission tomography is rapidly spreading not only because of its diagnostic power but also because of its robustness and the fact that interpreting amino acid uptake may be clearly easier than PW and DW images for clinicians involved in neuro-oncology, owing to the higher tumor-to-background contrast and more homogenous background [62]. However, most neuro-oncological centers have access to advanced MRI techniques and not to PET. Multimodal MRI requires substantial expertise to ensure meaningful assessment and is more prone to artifacts, therefore it is not always used efficiently. Other limitations are the lack of standardization for data acquisition and processing, which is likely to account -at least in part- for results conflicting PET. Of note, the applicability of modern MRI techniques is hindered by the presence of hemorrhage, which impedes their use in a non-negligible number of cases [119].

At the initial diagnosis of glioma, both modalities can help to define a site for biopsy, but amino acid PET appears to be somewhat more powerful in delineating the true extent of the tumor and guiding surgical excision. Regarding the preoperative assessment of tumor grade, both modalities are moderately accurate, but for PET there is room for improvement through dynamic acquisition and kinetic tracer analysis. Assessment of therapeutic efficacy can be achieved especially with amino acid PET, while the data for advanced MRI are sparse. As regards differentiation between true tumor progression or late recurrence from non-specific post-therapeutic pseudoprogression and radionecrosis, both methods have been found to be particularly helpful. The complemen-

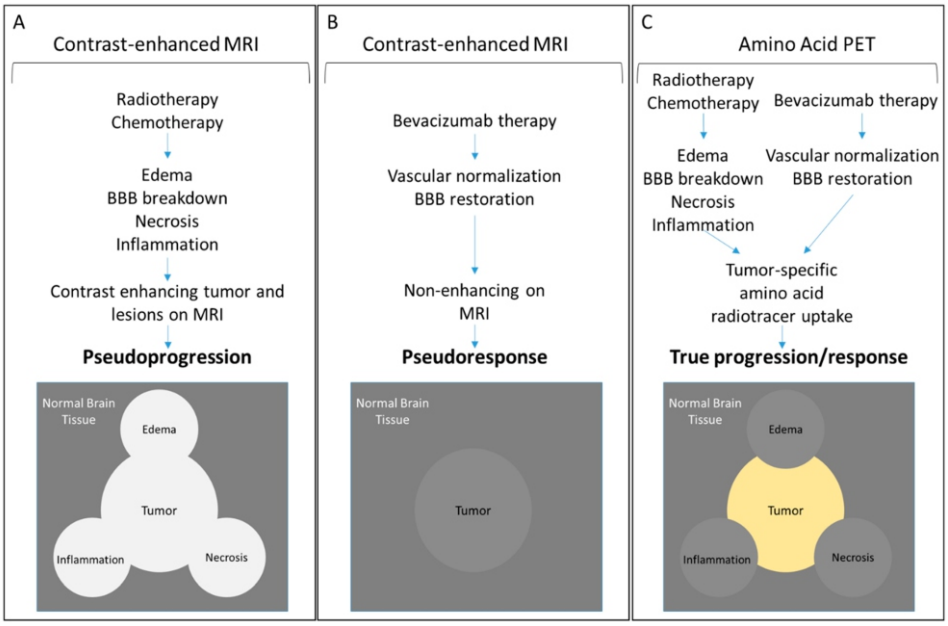

Figure 8. Representation of classic MRI and amino acid PET outcomes following the treatment of glioma. **A)** Radiochemotherapy can lead to edema, inflammation, BBB breakdown, and necrosis; these effects generate contrast-enhancing lesions that obscure true tumor boundaries and lead to pseudoprogression. **B)** Conversely, vascular normalization with BBB restoration following bevacizumab can diminish contrast enhancement and yield a false appearance of pseudoresponse to treatment, even without an associated true anti-tumor response. **C**) Amino acid PET reflects specific radiotracer accumulation within the cellular component of the tumor mass, thus revealing true tumor boundaries and immediate metabolic changes in response to therapy. Reproduced under a Creative Commons Attribution License CC BY 4.0 from copyright holders Amer M. Najjar and colleagues; Bioengineering, published by Multidisciplinary Digital Publishing Institute (MDPI), Basel, Switzerland, 2018 [8].

tary nature of the two modalities has to be explored in future comparative studies to further improve the diagnostics of brain tumors [120].

Standardization of multimodal MRI and PET imaging protocols and data processing for better comparability and easier reproducibility of the data is very likely to augment their clinical application. Existing and novel radiotracers with higher tumor specificity should increasingly be applied in clinical trials and large prospective cohort studies and compared with both advanced MRI techniques and with molecular biomarkers for the classification and management of brain tumors, in order to further clarify their value in clinical practice as diagnostic and prognostic tools.

The authors declare that they have no conflicts of interest.

Bibliography

1. McNeill KA. Epidemiology of brain tumors. *Neurol Clin* 2016; 34: 981-98.
2. Kleihues P, Cavenee W (Eds.) *Tumours of the nervous system: World Health Organization classification of tumours*. IARC Press, Lyon, France, 2000.
3. Louis DN, Perry A, Reifenberger G et al. The 2016 World Health Organization classification of tumors of the central nervous system: a summary. *Acta Neuropathol* 2016; 131: 803-20.
4. Stupp R, Mason WP, van den Bent MJ et al. Radiotherapy plus concomitant and adjuvant temozolomide for glioblastoma. *N Engl J Med* 2005; 352: 987-96.
5. Schnell O, Thorsteinsdottir J, Fleischmann DF et al. Re-irradiation strategies in combination with bevacizumab for recurrent malignant glioma. *J Neurooncol* 2016; 130: 591-9.
6. Weller M, van den Bent M, Hopkins K et al. EANO guideline for the diagnosis and treatment of anaplastic gliomas and glioblastoma. *Lancet Oncol* 2014; 15: e395-403.
7. Wong ET, Gautam S, Malchow C et al. Bevacizumab for recurrent glioblastoma multiforme: a meta-analysis. *J Natl Compr Canc Netw* 2011; 9: 403-7.
8. Najjar AM, Johnson JM, Schellingerhout D. The emerging role of amino acid PET in neuro-oncolgy. *Bioengineering (Basel)* 2018; 5: E104.
9. Fink JR, Muzi M, Peck M, Krohn KA. Continuing education: Multimodality brain tumor imaging - MRI, PET, and PET/MRI. *J Nucl Med* 2015; 56: 1554-61.
10. Montagne A, Toga AW, Zlokovic BV. Blood-brain barrier permeability and gadolinium: benefits and potential pitfalls in research. *JAMA Neurol* 2016; 73: 13-4.
11. Roberts HC, Roberts TP, Bollen AW et al. Correlation of microvascular permeability derived from dynamic contrast-enhanced MR imaging with histologic grade and tumor labeling index: a study in human brain tumors. *Acad Radiol* 2001; 8: 384-91.
12. Upadhyay N, Waldman AD. Conventional MRI evaluation of gliomas. *Br J Radiol* 2011; 84 Spec No 2: S107-11.
13. Lohmann P, Stavrinou P, Lipke K et al. FET PET reveals considerable spatial differences in tumour burden compared to conventional MRI in newly diagnosed glioblastoma. *Eur J Nucl Med Mol Imaging* 2019; 46: 591-602.
14. Knopp EA, Cha S, Johnson G et al. Glial neoplasms: dynamic contrast-enhanced T2*-weighted MR imaging. *Radiology* 1999; 211: 791-8.
15. Zaharchuk G. Theoretical basis of hemodynamic MR imaging techniques to measure cerebral blood volume, cerebral blood flow, and permeability. *Am J Neuroradiol* 2007; 28: 1850-8.
16. Tofts PS. Modeling tracer kinetics in dynamic Gd-DTPA MR imaging. *J Magn Reson Imaging* 1997; 7: 91-101.
17. Le Bihan D, Breton E, Lallemand D et al. MR imaging of intravoxel incoherent motions: application to diffusion and perfusion in neurologic disorders. *Radiology* 1986; 161: 401-7.

18. Koh DM, Padhani AR. Diffusion-weighted MRI: a new functional clinical technique for tumour imaging. *Br J Radiol* 2006; 79: 633-5.
19. Langen KJ, Galldiks N, Hattingen E et al. Advances in neuro-oncology imaging. *Nat Rev Neurol* 2017; 13: 279-89.
20. Kono K, Inoue Y, Nakayama K et al. The role of diffusion-weighted imaging in patients with brain tumors. *Am J Neuroradiol* 2001; 22: 1081-8.
21. Chang SC, Lai PH, Chen WL et al. Diffusion-weighted MRI features of brain abscess and cystic or necrotic brain tumors: comparison with conventional MRI. *Clin Imaging* 2002; 26: 227-36.
22. Pope WB, Lai A, Mehta R et al. Apparent diffusion coefficient histogram analysis stratifies progression-free survival in newly diagnosed bevacizumab-treated glioblastoma. *Am J Neuroradiol* 2011; 32: 882-9.
23. Pope WB, Qiao XJ, Kim H et al. Apparent diffusion coefficient histogram analysis stratifies progression-free and overall survival in patients with recurrent GBM treated with bevacizumab: a multi-center study. *J Neurooncol* 2012; 108: 491-8.
24. Basser PJ, Pierpaoli C. Microstructural and physiological features of tissues elucidated by quantitative-diffusion-tensor MRI. *J Magn Reson B* 1996; 111: 209-19.
25. Price SJ, Jena R, Burnet NG et al. Improved delineation of glioma margins and regions of infiltration with the use of diffusion tensor imaging: an image-guided biopsy study. *Am J Neuroradiol* 2006; 27: 1969-74.
26. White ML, Zhang Y, Yu F, Jaffar Kazmi SA. Diffusion tensor MR imaging of cerebral gliomas: evaluating fractional anisotropy characteristics. *Am J Neuroradiol* 2011; 32: 374-81.
27. Byrnes TJ, Barrick TR, Bell BA, Clark CA. Diffusion tensor imaging discriminates between glioblastoma and cerebral metastases in vivo. *NMR Biomed* 2011; 24: 54-60.
28. Bagadia A, Purandare H, Misra BK, Gupta S. Application of magnetic resonance tractography in the perioperative planning of patients with eloquent region intra-axial brain lesions. *J Clin Neurosci* 2011; 18: 633-9.
29. Howe FA, Barton SJ, Cudlip SA et al. Metabolic profiles of human brain tumors using quantitative in vivo 1H magnetic resonance spectroscopy. *Magn Reson Med* 2003; 49: 223-32.
30. Kwock L, Smith JK, Castillo M et al. Clinical applications of proton MR spectroscopy in oncology. *Technol Cancer Res Treat* 2002; 1: 17-28.
31. Negendank WG, Sauter R, Brown TR et al. Proton magnetic resonance spectroscopy in patients with glial tumors: a multicenter study. *J Neurosurg* 1996; 84: 449-58.
32. Glunde K, Bhujwalla ZM, Ronen SM. Choline metabolism in malignant transformation. *Nat Rev Cancer* 2011; 11: 835-48.
33. Nelson SJ. Multivoxel magnetic resonance spectroscopy of brain tumors. *Mol Cancer Ther* 2003; 2: 497-507.
34. Rabinov JD, Lee PL, Barker FG et al. In vivo 3-T MR spectroscopy in the distinction of recurrent glioma versus radiation effects: Initial experience. *Radiology* 2002; 225: 871-9.
35. van Dijken BRJ, van Laar PJ, Holtman GA, van der Hoorn A. Diagnostic accuracy of magnetic resonance imaging techniques for treatment response evaluation in patients with high-grade glioma, a systematic review and meta-analysis. *Eur Radiol* 2017; 27: 4129-44.
36. Alexiou GA, Tsiouris S, Voulgaris S et al. Glioblastoma multiforme imaging: the role of nuclear medicine. *Curr Radiopharm* 2012; 5: 308-13.
37. Lopci E, Franzese C, Grimaldi M, et al. Imaging biomarkers in primary brain tumours. *Eur J Nucl Med Mol Imaging* 2015; 42: 597-612.
38. Krohn KA, Mankoff DA, Muzi M et al. True tracers: comparing FDG with glucose and FLT with thymidine. *Nucl Med Biol* 2005; 32: 663-71.
39. Spence AM, Muzi M, Mankoff DA et al. ^{18}F-FDG PET of gliomas at delayed intervals: improved distinction between tumor and normal gray matter. *J Nucl Med* 2004; 45: 1653-9.
40. Delbeke D, Meyerowitz C, Lapidus RL et al. Optimal cutoff levels of F-18 fluorodeoxyglucose uptake in the differentiation of low-grade from high-grade brain tumors with PET. *Radiology* 1995; 195: 47-52.
41. Padma MV, Said S, Jacobs M et al. Prediction of pathology and survival by FDG PET in gliomas. *J Neurooncol* 2003; 64: 227-37.
42. Nihashi T, Dahabreh IJ, Terasawa T. Diagnostic accuracy of PET for recurrent glioma diagnosis: a meta-analysis. *Am J Neuroradiol* 2013; 34: 944-50.
43. Ricci PE, Karis JP, Heiserman JE et al. Differentiating recurrent tumor from radiation necrosis: time for re-evaluation of positron emission tomography? *Am J Neuroradiol* 1998; 19: 407-13.
44. Galldiks N, Langen KJ, Pope WB. From the clinician's point of view-What is the status quo of positron emission tomography in patients with brain tumors? *Neuro Oncol* 2015; 17: 1434-44.
45. Molecular structures of amino acid PET tracers retrieved from PubChem, the open chemistry database at the National Institutes of Health (NIH): https://pubchem.ncbi.nlm.nih.gov, on 2019-9-28.
46. Wienhard K, Herholz K, Coenen HH et al. Increased amino acid transport into brain tumors measured by PET of L-(2-^{18}F) fluorotyrosine. *J Nucl Med* 1991; 32: 1338-46.
47. Herholz K. Brain tumors: an update on clinical PET research in gliomas. *Semin Nucl Med* 2017; 47: 5-17.
48. Singhal T, Narayanan TK, Jain V et al. ^{11}C-L-methionine positron emission tomography in the clinical management of cerebral gliomas. *Mol Imaging Biol* 2008; 10: 1-18.
49. Cicone F, Filss CP, Minniti G et al. Volumetric assessment of recurrent or progressive gliomas: comparison between F-DOPA PET and perfusion-weighted MRI. *Eur J Nucl Med Mol Imaging* 2015; 42: 905-15.
50. Shields AF, Grierson JR, Dohmen BM et al. Imaging proliferation in vivo with [F-18] FLT and positron emission tomography. *Nat Med* 1998; 4: 1334-6.
51. Rasey JS, Grierson JR, Wiens LW et al. Validation of FLT uptake as a measure of thymidine kinase-1 activity in A549 carcinoma cells. *J Nucl Med* 2002; 43: 1210-7.
52. Shinomiya A, Kawai N, Okada M et al. Evaluation of 3'-deoxy-3'-[^{18}F]-fluorothymidine (^{18}F-FLT) kinetics correlated with thymidine kinase-1 expression and cell proliferation in newly diagnosed gliomas. *Eur J Nucl Med Mol Imaging* 2013; 40: 175-85.
53. Nowosielski M, DiFranco MD, Putzer D et al. An intra-individual comparison of MRI, [^{18}F]-FET and [^{18}F]-FLT PET in patients with high-grade gliomas. *PLoS One* 2014; 9: e95830.
54. Muzi M, Spence AM, O'Sullivan F et al. Kinetic analysis of 3'-deoxy-3'-18F-fluorothymidine in patients with gliomas. *J Nucl Med* 2006; 47: 1612-21.
55. Giovannini E, Lazzeri P, Milano A et al. Clinical applications of choline PET/CT in brain tumors. *Curr Pharm Des* 2015; 21: 121-7.
56. Spaeth N, Wyss MT, Pahnke J et al. Uptake of ^{18}F-fluorocholine, ^{18}F-fluoro-ethyl-L-tyrosine and ^{18}F-fluoro-2-deoxyglucose in F98 gliomas in the rat. *Eur J Nucl Med Mol Imaging* 2006; 33: 673-82.
57. Henriksen G, Herz M, Hauser A et al. Synthesis and preclinical evaluation of the choline transport tracer deshydroxy-[^{18}F] fluorocholine ([^{18}F]dOC). *Nucl Med Biol* 2004; 31: 851-8.
58. Quartuccio N, Asselin MC. The validation path of hypoxia PET imaging: focus on brain tumours. *Curr Med Chem* 2018; 25: 3074-95.
59. Cher LM, Murone C, Lawrentschuk N et al. Correlation of hypoxic cell fraction and angiogenesis with glucose metabolic rate in gliomas using ^{18}F-fluoromisonidazole, ^{18}F-FDG PET, and immunohistochemical studies. *J Nucl Med* 2006; 47: 410-8.
60. Suchorska B, Tonn JC, Jansen NL. PET imaging for brain tumor diagnostics. *Curr Opin Neurol* 2014; 27: 683-8.
61. Albert NL, Weller M, Suchorska B et al. Response Assessment in Neuro-Oncology working group and European Association for Neuro-Oncology recommendations for the clinical use of PET imaging in gliomas. *Neuro Oncol* 2016; 18: 1199-208.
62. Filss CP, Cicone F, Shah NJ et al. Amino acid PET and MR perfusion imaging in brain tumours. *Clin Transl Imaging* 2017; 5: 209-23.
63. Vöglein J, Tüttenberg J, Weimer M et al. Treatment monitoring in gliomas: comparison of dynamic susceptibility-weighted contrast-enhanced and spectroscopic MRI techniques for identifying

treatment failure. I*nvest Radiol* 2011; 46: 390-400.
64. Hutterer M, Nowosielski M, Putzer D et al. [F-18]-fluoro-ethyl-L-tyrosine PET: a valuable diagnostic tool in neuro-oncology, but not all that glitters is glioma. *Neuro Oncol* 2013; 15: 341-51.
65. Floeth FW, Pauleit D, Wittsack HJ et al. Multimodal metabolic imaging of cerebral gliomas: positron emission tomography with [^{18}F]fluoroethyl-L-tyrosine and magnetic resonance spectroscopy. *J Neurosurg* 2005; 102: 318-27.
66. Näslund O, Smits A, Förander P et al. Amino acid tracers in PET imaging of diffuse low-grade gliomas: a systematic review of preoperative applications. *Acta Neurochir (Wien)* 2018; 160:1451-60.
67. Langen KJ, Galldiks N. Update on amino acid PET of brain tumours. *Curr Opin Neurol* 2018; 31: 354-61.
68. Manabe O, Hattori N, Yamaguchi S et al. Oligodendroglial component complicates the prediction of tumour grading with metabolic imaging. *Eur J Nucl Med Mol Imaging* 2015; 42: 896-904.
69. Jansen NL, Suchorska B, Wenter V et al. Prognostic significance of dynamic ^{18}F-FET PET in newly diagnosed astrocytic high-grade glioma. *J Nucl Med* 2015; 56: 9-15.
70. Calcagni ML, Galli G, Giordano A et al. Dynamic O-(2-[^{18}F]fluoroethyl)-L-tyrosine (F-18 FET) PET for glioma grading: assessment of individual probability of malignancy. *Clin Nucl Med* 2011; 36: 841-7.
71. Toyooka M, Kimura H, Uematsu H et al. Tissue characterization of glioma by proton magnetic resonance spectroscopy and perfusion-weighted magnetic resonance imaging: glioma grading and histological correlation. *Clin Imaging* 2008; 32: 251-8.
72. Arvinda HR, Kesavadas C, Sarma PS et al. Glioma grading: sensitivity, specificity, positive and negative predictive values of diffusion and perfusion imaging. *J Neurooncol* 2009; 94: 87-96.
73. Hilario A, Ramos A, Perez-Nunez A et al. The added value of apparent diffusion coefficient to cerebral blood volume in the preoperative grading of diffuse gliomas. *Am J Neuroradiol* 2012; 33: 701-7.
74. Lev MH, Ozsunar Y, Henson JW et al. Glial tumor grading and outcome prediction using dynamic spin-echo MR susceptibility mapping compared with conventional contrast-enhanced MR: confounding effect of elevated rCBV of oligodendrogliomas. *Am J Neuroradiol* 2004; 25: 214-21.
75. Smits A, Baumert BG. The clinical value of PET with amino acid tracers for gliomas WHO Grade II. *Int J Mol Imaging* 2011; 2011: 372-509.
76. Villani V, Carapella CM, Chiaravalloti A et al. The role of PET [^{18}F]FDOPA in evaluating low-grade glioma. *Anticancer Res* 2015; 35: 5117-22.
77. Suchorska B, Jansen NL, Linn J et al. Biological tumor volume in ^{18}FET-PET before radiochemotherapy correlates with survival in GBM. *Neurology* 2015; 84: 710-9.
78. Piroth MD, Pinkawa M, Holy R et al. Prognostic value of early [^{18}F]fluoroethyltyrosine positron emission tomography after radiochemotherapy in glioblastoma multiforme. *Int J Radiat Oncol Biol Phys* 2011; 80: 176-84.
79. Schmainda KM, Zhang Z, Prah M et al. Dynamic susceptibility contrast MRI measures of relative cerebral blood volume as a prognostic marker for overall survival in recurrent glioblastoma: results from the ACRIN 6677/RTOG 0625 multicenter trial. *Neuro Oncol* 2015; 178: 1148-56.
80. Jain R, Poisson L, Narang J et al. Genomic mapping and survival prediction in glioblastoma: molecular subclassification strengthened by hemodynamic imaging biomarkers. *Radiology* 2013; 267: 212-20.
81. Rieken S, Habermehl D, Giesel FL et al. Analysis of FET-PET imaging for target volume definition in patients with gliomas treated with conformal radiotherapy. *Radiother Oncol* 2013; 109: 487-92.
82. Munck P, Rosenschold AF, Costa J et al. Impact of [^{18}F]-fluoro-ethyl-tyrosine PET imaging on target definition for radiation therapy of high-grade glioma. *Neuro Oncol* 2015; 17: 757-63.
83. Matsuo M, Miwa K, Tanaka O et al. Impact of [^{11}C]methionine positron emission tomography for target definition of glioblastoma multiforme in radiation therapy planning. *Int J Radiat Oncol Biol Phys* 2012; 82: 83-9.
84. Blasel S, Franz K, Ackermann H et al. Stripe-like increase of rCBV beyond the visible border of glioblastomas: site of tumor infiltration growing after neurosurgery. *J Neurooncol* 2011; 103: 575-84.
85. Rose S, Fay M, Thomas P et al. Correlation of MRI-derived apparent diffusion coefficients in newly diagnosed gliomas with [^{18}F]-fluoro-L-dopa PET: What are we really measuring with minimum ADC? *Am J Neuroradiol* 2013; 34: 758-64.
86. Popp I, Bott S, Mix M et al. Diffusion-weighted MRI and ADC versus FET-PET and GdT1w-MRI for gross tumor volume (GTV) delineation in re-irradiation of recurrent glioblastoma. *Radiother Oncol* 2019; 130: 121-31.
87. Choi H, Paeng JC, Cheon GJ et al. Correlation of ^{11}C-methionine PET and diffusion-weighted MRI: Is there a complementary diagnostic role for gliomas? *Nucl Med Commun* 2014; 35: 720-6.
88. Stadlbauer A. Prante O, Nimsky C et al. Metabolic imaging of cerebral gliomas: Spatial correlation of changes in O-(2-^{18}F-fluoroethyl)-L-tyrosine PET and proton magnetic resonance spectroscopic imaging. *J Nucl Med* 2008; 49: 721-9.
89. Mauler J, Maudsley AA, Langen KJ et al. Spatial relationship of glioma volume derived from ^{18}F-FET PET and volumetric MR spectroscopy imaging: a hybrid PET/MRI study. *J Nucl Med* 2018; 59: 603-9.
90. Plotkin M, Blechschmidt C, Auf G et al. Comparison of F-18 FET-PET with F-18 FDG-PET for biopsy planning of non-contrast-enhancing gliomas. *Eur Radiol* 2010; 20: 2496-502.
91. Pirotte B, Goldman S, Massager N et al. Combined use of ^{18}F-fluorodeoxyglucose and ^{11}C-methionine in 45 positron emission tomography-guided stereotactic brain biopsies. *J Neurosurg* 2004; 101: 476-83.
92. Sadeghi N, Salmon I, Decaestecker C et al. Stereotactic comparison among cerebral blood volume, methionine uptake, and histopathology in brain glioma. *Am J Neuroradiol* 2007; 28: 455-61.
93. Berntsson SG, Falk A, Savitcheva I et al. Perfusion and diffusion MRI combined with ^{11}C-methionine PET in the preoperative evaluation of suspected adult low-grade gliomas. *J Neurooncol* 2013; 114: 241-9.
94. Filss CP, Galldiks N, Stoffels G et al. Comparison of ^{18}F-FET PET and perfusion-weighted MR imaging: a PET/MR imaging hybrid study in patients with brain tumors. *J Nucl Med* 2014; 55: 540-5.
95. Roelcke U, Wyss MT, Nowosielski M et al. Amino acid positron emission tomography to monitor chemotherapy response and predict seizure control and progression-free survival in WHO grade II gliomas. *Neuro Oncol* 2016; 18: 744-51.
96. Wyss M, Hofer S, Bruehlmeier M et al. Early metabolic responses in temozolomide treated low-grade glioma patients. *J Neurooncol* 2009; 95: 87-93.
97. Galldiks N, Rapp M, Stoffels G et al. Response assessment of bevacizumab in patients with recurrent malignant glioma using [^{18}F]fluoroethyl-L-tyrosine PET in comparison to MRI. *Eur J Nucl Med Mol Imaging* 2013; 40: 22-33.
98. Schwarzenberg J, Czernin J, Cloughesy TF et al. Treatment response evaluation using ^{18}F-FDOPA PET in patients with recurrent malignant glioma on bevacizumab therapy. *Clin Cancer Res* 2014; 20: 3550-9.
99. Brandsma D, Stalpers L, Taal W et al. Clinical features, mechanisms, and management of pseudoprogression in malignant gliomas. *Lancet Oncol* 2008; 9: 453-61.
100. Galldiks N, Dunkl V, Stoffels G et al. Diagnosis of pseudoprogression in patients with glioblastoma using O-(2-[^{18}F]fluoroethyl)-L-tyrosine PET. *Eur J Nucl Med Mol Imaging* 2015; 42: 685-95.
101. Suh CH, Kim HS, Choi YJ et al. Prediction of pseudoprogression in patients with glioblastomas using the initial and final area under the curves ratio derived from dynamic contrast-enhanced T1-weighted perfusion MR imaging. *Am J Neuroradiol* 2013; 34: 2278-86.
102. Patel P, Baradaran H, Delgado D et al. MR perfusion-weighted imaging in the evaluation of high-grade gliomas after treatment: a systematic review and meta-analysis. *Neuro Oncol* 2017;

9: 118-27.
103. Herrmann K, Czernin J, Cloughesy T et al. Comparison of visual and semiquantitative analysis of ^{18}F-FDOPA-PET/CT for recurrence detection in glioblastoma patients. *Neuro Oncol* 2014; 16: 603-9.
104. D'Souza MM, Sharma R, Jaimini et al. ^{11}C-MET PET/CT and advanced MRI in the evaluation of tumor recurrence in high-grade gliomas. *Clin Nucl Med* 2014; 39: 791-8.
105. Sharma R, D'Souza M, Jaimini A et al. A comparison study of ^{11}C-methionine and ^{18}F-fluorodeoxyglucose positron emission tomography-computed tomography scans in evaluation of patients with recurrent brain tumors. *Indian J Nucl Med* 2016; 31: 93-102.
106. Kim YH, Oh SW, Lim YJ et al. Differentiating radiation necrosis from tumor recurrence in high-grade gliomas: assessing the efficacy of ^{18}F-FDG PET, ^{11}C-methionine PET and perfusion MRI. *Clin Neurol Neurosurg* 2010; 112: 758-65.
107. Dandois V, Rommel D, Renard L et al. Substitution of ^{11}C-methionine PET by perfusion MRI during the follow-up of treated high-grade gliomas: preliminary results in clinical practice. *J Neuroradiol* 2010; 37: 89-97.
108. Karavaeva E, Harris RJ, Leu K et al. Relationship between [^{18}F]FDOPA PET uptake, apparent diffusion coefficient (ADC), and proliferation rate in recurrent malignant gliomas. *Mol Imaging Biol* 2015; 17: 434-42.
109. Pyka T, Hiob D, Preibisch C et al. Diagnosis of glioma recurrence using multiparametric dynamic ^{18}F-fluoroethyl-tyrosine PET-MRI. *Eur J Radiol* 2018; 103: 32-7.
110. Bailey DL, Antoch G, Bartenstein P et al. Combined PET/MR: the real work has just started. Summary report of the Third International Workshop on PET/MR imaging; February 17-21, 2014, Tübingen, Germany. *Mol Imaging Biol* 2015; 17: 297-312.
111. Widhalm G, Krssak M, Minchev G et al. Value of ^{1}H-magnetic resonance spectroscopy chemical shift imaging for detection of anaplastic foci in diffusely infiltrating gliomas with non-significant contrast-enhancement. *J Neurol Neurosurg Psychiatry* 2011; 82: 512-20.
112. Mauler J, Maudsley AA, Langen KJ et al. Spatial relationship of glioma volume derived from ^{18}F-FET PET and volumetric MR spectroscopy imaging: a hybrid PET/MRI study. *J Nucl Med* 2018; 59: 603-9.
113. Weber MA, Henze M, Tuttenberg J et al. Biopsy targeting gliomas: do functional imaging techniques identify similar target areas? *Invest Radiol* 2010; 45: 755-68.
114. Preuss M, Werner P, Barthel H et al. Integrated PET/MRI for planning navigated biopsies in pediatric brain tumors. *Childs Nerv Syst* 2014; 30: 1399-403.
115. Gauvain K, Ponisio MR, Barone A et al. ^{18}F-FDOPA PET/MRI for monitoring early response to bevacizumab in children with recurrent brain tumors. *Neurooncol Pract* 2018; 5: 28-36.
116. Pichler BJ, Kolb A, Nägele T, Schlemmer HP. PET/MRI: paving the way for the next generation of clinical multimodality imaging applications. *J Nucl Med* 2010; 51: 333-6.
117. Fleischmann DF, Unterrainer M, Corradini S et al. Report of first recurrent glioma patients examined with PET-MRI prior to re-irradiation. *PLoS One* 2019; 14: e0216111.
118. Deuschl C, Kirchner J, Poeppel TD. ^{11}C-MET PET/MRI for detection of recurrent glioma. *Eur J Nucl Med Mol Imaging* 2018; 45: 593-601.
119. Heo YJ, Kim HS, Park JE et al. Uninterpretable dynamic susceptibility contrast-enhanced perfusion MR images in patients with post-treatment glioblastomas: cross-validation of alternative imaging options. *PLoS One* 2015; 10: e0136380.
120. Huang RY, Neagu MR, Reardon DA, Wen PY. Pitfalls in the neuroimaging of glioblastoma in the era of antiangiogenic and immuno/targeted therapy-detecting illusive disease, defining response. *Front Neurol* 2015; 6: 33.